Field-induced magnetic transition and spin fluctuations in the quantum spin-liquid candidate CsYbSe_{2}

Jie Xing, Liurukara D. Sanjeewa, Jungsoo Kim, G. R. Stewart, Andrey Podlesnyak, and Athena S. Sefat

Phys. Rev. B **100**, 220407 — Published 16 December 2019

DOI: 10.1103/PhysRevB.100.220407

Field-induced magnetic transition and spin fluctuation in quantum spin liquid candidate $CsYbSe_2$

Jie Xing,[1] Liurukara D. Sanjeewa,[1] Jungsoo Kim,[2] G. R. Stewart,[2] Andrey Podlesnyak,[3] and Athena S. Sefat[1]

[1] *Materials Science and Technology Division, Oak Ridge National Laboratory, Oak Ridge, Tennessee 37831, USA*
[2] *Department of Physics, University of Florida, Gainesville, Florida 32611, USA*
[3] *Neutron Scattering Division, Oak Ridge National Laboratory, Oak Ridge, TN 37831*

(Dated: December 4, 2019)

Two-dimensional triangular-lattice materials with spin-1/2 are perfect platforms for investigating quantum frustrated physics with spin fluctuations. Here we report the structure, magnetization, heat capacity and inelastic neutron scattering (INS) results on cesium ytterbium diselenide, $CsYbSe_2$. There is no long-range magnetic order down to 0.4 K at zero field. The temperature dependent magnetization, $M(T)$, reveals an easy-plane magnetic anisotropy. A maximum is found in $M(T)$ around $T\sim$1.5 K when magnetic field H is applied in the ab plane, indicating the short-range interaction. The low-temperature isothermal magnetization $M(H)$ shows a one-third plateau of the estimated saturation moment, which is characteristic of a two-dimensional frustrated triangular lattice. Heat capacity shows field-induced long-range magnetic order for both $H||c$ and $H||ab$ directions. The broad peak in heat capacity and highly damped INS magnetic excitation at T=2 K suggests strong spin fluctuations. The dispersive in-plane INS, centered at the (1/3 1/3 0) point, and the absence of dispersion along c direction suggest 120° non-collinear 2D-like spin correlations. All these results indicate that the two-dimensional frustrated material $CsYbSe_2$ can be in proximity to the triangular-lattice quantum spin liquid. We propose an experimental low-temperature H-T phase diagram for $CsYbSe_2$.

I. INTRODUCTION

Frustrated magnetism is a challenge and intriguing field in the condensed matter physics due to multiple unconventional phenomena having ground state degeneracy [1, 2]. One important topic is the quantum spin liquid (QSL) state, where highly entangled spins prevent the breaking of any symmetry, even at zero temperature [3–5]. The spin interactions are restricted by the low-dimensional structure, which could enhance the spin fluctuations [2]. Until now, most QSL candidates are proposed in the low-spin S=1/2 frustrated systems, such as A_2IrO_3 (A=Na, Li, Cu), $H_3LiIr_2O_6$, κ-(BEDT-TTF)$_2$Cu$_2$(CN)$_3$, EtMe$_3$Sb[Pd(dmit)$_2$]$_2$, and $RuCl_3$ [6–20].

The rare-earth materials attract attention in searching for QSL candidates, as an alternative to Cu-based S=1/2 systems. The rare-earth ions with the odd number of 4f electrons could be treated as Kramers doublets with an effective spin $S_{\rm eff}$=1/2. Especially a number of Yb-based quantum magnets have attracted considerable interest, like the realization of a quantum spin S=1/2 chain in $YbAlO_3$ [21–23], and a quantum dimer magnet $Yb_2Si_2O_7$ [24]. Another Yb-base compound, $YbMgGaO_4$, was proposed as a QSL candidate with the frustrated Yb^{3+} triangular lattice. The heat capacity, magnetization, thermal conductivity, neutron scattering and muon spin relaxation find no transition in this compound and suggest a possible gapless QSL ground state [25–32]. However, the intrinsic Mg/Ga disorder exists between the frustrated layer and could induce the system to other states [25, 29, 30, 33–36].

Another classic 112 system ARQ_2 (A=Alkali metal, R=Rare-earth elements, Q= O, S, Se) was proposed as QSL candidate [37]. This 112 system is unique with the perfect rare-earth triangular layers, which are separated by the alkali metal ions. The distance of the nearest neighbor (NN) rare-earth ions and interlayer distance could be tuned by replacing the different A^+ and Q^{2-} ions. There is no structural or magnetic transition in NaYbCh_2 (Ch=O, S, Se) polycrystalline down to 50 mK [37]. The quantum chemistry calculation suggests that the Yb^{3+} $4f^{13}$ configuration should show large g_{ab} factors within the frustrated magnetic layers [38]. Electron spin resonance and magnetization reveal $S_{\rm eff}$=1/2 ground state at low temperature in the $NaYbS_2$ [39]. Until now, the investigation of the 112 system mostly focuses on the NaYbQ_2 compounds with the rhombohedral lattice (space group $R\bar{3}m$).

Magnetic fields perturb the quantum disordered ground state and induce the long-range order up-up-down spin state in $NaYbO_2$ [40–42]. This field-induced quantum phase transition, evoking alternative ground states, is an intriguing phenomenon in the frustrated triangular system. Two-dimensional triangular-lattice Heisenberg antiferromagnet could present several ground states under different fields due to degeneracy, such as 120° spin state, or collinear up-up-down state [43, 44]. In the easy-plane scenario, the up-up-down state could induce a plateau at one-third of the saturation magnetization due to the spin fluctuations [45], as it was found in the Cs_2CuBr_4, $CuFeO_2$, $Ba_3CoNb_2O_9$ and $Ba_3CoSb_2O_9$ [46–50]. The phase diagrams in the quantum scenario are not well elucidated, which inspires us to investigate more triangular-lattice compounds with different environments.

Here, we study another triangular lattice material $CsYbSe_2$. We present the detailed measurements of the

single crystal magnetization, heat capacity and inelastic neutron scattering (INS). There is no long-range order in the magnetization and heat capacity down to T=0.4 K at zero field, while large anisotropy is found between the ab plane and the c axis. The magnetic field induces a one-third plateau in the isothermal magnetization below H<7 T. Zero-field heat capacity suggests the QSL state in the triangular Heisenberg lattice. The low-temperature heat capacity with magnetic fields confirms the quantum-induced magnetic ordering in intermediate fields. The excitation spectra obtained from INS unambiguously demonstrate a quasi-2D nature of frustrated Yb^{3+} with $S_{\rm eff}$=1/2 in this triangular lattice.

II. MATERIALS AND METHODS

Millimeter-sized hexagonal shape $CsYbSe_2$ single crystals were synthesized by salt flux method following the procedure described in Ref. [51]. The energy-dispersive x-ray spectroscopy (EDS) shows the molar ratio of Cs:Yb:Se is close to 1:1:2. Fig 1(a) demonstrates the structure and the optical microscope image of $CsYbSe_2$. X-ray diffraction (XRD) was collected on a PANalytical X'pert Pro diffractometer equipped with an incident beam monochromator (Cu Kα_1 radiation) at room temperature [Fig. 1(c)]. Sharp (00l) peaks suggest good crystalline quality in the single crystal.

Magnetic properties were measured using a Quantum Design (QD) Magnetic Properties Measurement System (MPMS3). The magnetization below 2 K was measured by the MPMS3 iHe3 option. The total mass of the measured crystals was ∼3 mg. Temperature dependent heat capacity was measured in QD Physical Properties Measurement System (PPMS) using the relaxation technique. The mass of the single crystals for heat capacity was ∼2 mg.

Neutron scattering measurements of $CsYbSe_2$ were performed at the time-of-flight Cold Neutron Chopper Spectrometer (CNCS) [52, 53], at the Spallation Neutron Source at Oak Ridge National Laboratory. Data were collected with 12 single crystal samples of total mass ∼0.1 g, which were co-aligned to within 2° using a Multiwire x-ray Laue machine in the (HHL) scattering plane. The measurements were carried out using the rotating single crystal method at a temperature of T = 2 K. The data were collected using fixed incident neutron energies of E_i = 3.32 meV and E_i = 25.0 meV resulting in a full-width-at-half-maximum energy resolution of 0.07 meV and 0.75 meV at the elastic position, respectively. All time-of-flight data-sets were combined to produce a four-dimensional scattering-intensity function $I(\mathbf{Q}, E_f)$, where $\mathbf{Q}$ is the momentum transfer and E_f is the energy transfer. For data reduction and analysis, we used the MANTID [54] and HORACE [55] software packages.

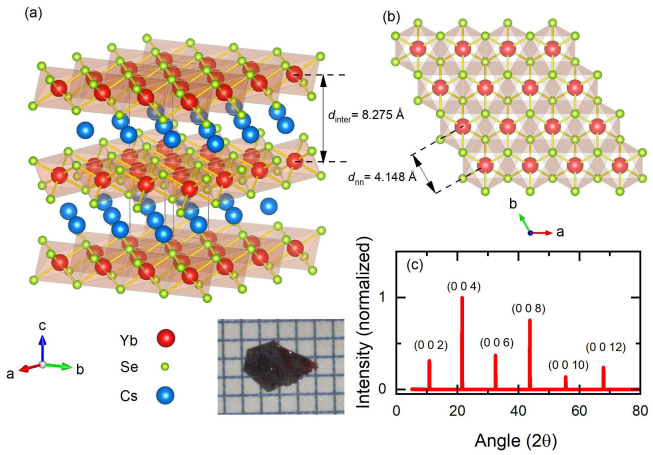

FIG. 1. (a) The structure of $CsYbSe_2$. The distance between the nearest two dimensional Yb triangular layers is 8.275 Å. (b) The perfect frustrated Yb triangular layer. The distance of the nearest neighbor Yb ions is 4.148 Å. Each Yb ion is connected to six nearest Yb ions via six Yb-Se-Yb bonds. (c) The X-ray diffraction pattern obtained on the surface of a single crystal.

III. RESULTS AND DISCUSSION

Unlike $NaYbO_2$, which is crystallized in $R\bar{3}m$ space group, $CsYbSe_2$ adopts $P6_3/mmc$ space group due to different layer stacking sequences. Because the large radius of Cs ions, two layers of YbSeYb are packed in $CsYbSe_2$ along the c axis while three layers of Yb-O-Yb are packed in $NaYbO_2$. $CsYbSe_2$ has similar ideal triangular layers of Yb^{3+} in the $YbSe_6$ octahedral environment, as shown in Fig. 1(b). The distance between Yb-layers $d_{\rm inter}$ in $CsYbSe_2$ is 8.275 Å, which is larger than the $d_{\rm inter}$ in $NaYbO_2$ and comparable to $d_{\rm inter}$ in $YbMgGaO_4$. The distance between the nearest neighbor Yb^{3+} $d_{\rm NN}$ is 4.148 Å, which is slightly larger than $d_{\rm NN}$ in $NaYbO_2$ and $NaYbS_2$ due to the larger size of Se ion. The 2D ratio $d_{\rm inter}/d_{\rm NN}$ = 2 varies from 1.6 for $NaYbO_2$ to 2.47 for $YbMgGaO_4$. This difference between the 2D ratio reflects on the different field-induced magnetic transitions at low temperatures in $NaYbO_2$ and $YbMgGaO_4$ [32, 41, 42]. Based on two-dimensional $CsYbSe_2$ structure, it inspires us to investigate the details of magnetic properties using the single crystals.

A. Magnetization

The DC susceptibility measurements under H=1 T [Fig. 2(a)] show no evidence of a magnetic transition in the $CsYbSe_2$ down to 2 K. We used Curie-Weiss law to fit the magnetization, in both field directions, for the temperatures above 250 K and around 10 K [Fig. 2(a)]. The effective magnetic moment $\mu_{\rm eff}$ was evaluated us-

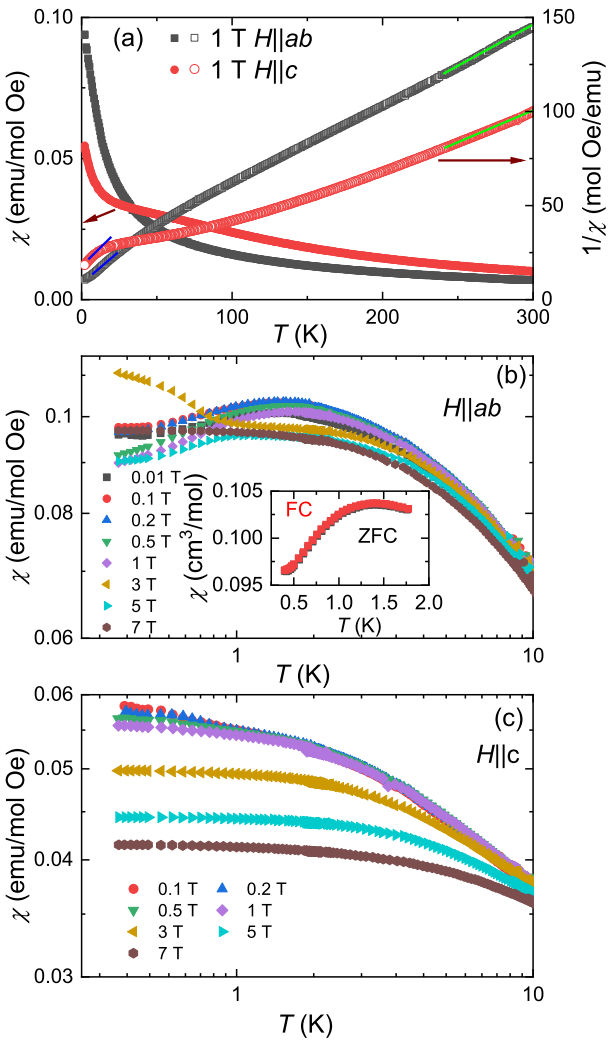

FIG. 2. (a) The temperature dependence of DC susceptibility for the $CsYbSe_2$ single crystal in the ab plane and along the c axis. Solid lines show the fit to the Curie-Weiss law, see the text and Table I. (b,c) The temperature dependence of magnetic susceptibility in different magnetic fields $H||ab$ (b) $H||c$ (c). The discontinued points around 1.8 K are due to the different temperature control method of the measurement. Inset of (b) shows the low temperature field cooled (FC) and zero field cooled (ZFC) susceptibility at H=0.2 T.

ing the Curie constant from the fits. The Curie-Weiss temperature θ_{CW} and $\mu_{\rm eff}$ are shown in Table I. The effective moment is close to the moment of free Yb^{3+} (4.54 $\mu_{\rm B}$) at high temperatures. As the temperature decreases, the effective moment also decreases and exhibits strong anisotropic behavior, similar to that found in $NaYbS_2$ [39]. In the anisotropic two dimensional Heisenberg system, the average magnetic susceptibility is described by $\chi_{avg} = (2\chi_{ab} + \chi_c)/3$ [26]. The negative value $\theta_{avg} = -16.9$ K from Curie-Weiss fitting at low temperature indicates the antiferromagnetic interaction between Yb^{3+} ions. Interestingly, this value is slightly lower than $\theta = -10.3$ K in the similar Yb-triangular lattice material $NaYbO_2$, although the $d_{\rm NN}$ in $CsYbSe_2$ is longer than $d_{\rm NN}$ in $NaYbO_2$.

TABLE I. The effective magnetic moment ($\mu_{\rm eff}$) and Curie-Weiss temperature (θ_{CW}) obtained from the fit at high temperatures (HT) of $250-300$ K, and at low temperatures (LT) of $8-12$ K.

	$\mu_{\rm eff}[\mu_{\rm B}]$ HT	θ_{CW}[K] HT	$\mu_{\rm eff}[\mu_{\rm B}]$ LT	θ_{CW}[K] LT
$H\|\|ab$	4.34	-42.3	3.48	-13.2
$H\|\|c$	4.88	-31.6	3.26	-26.1

The low-temperature part of the DC susceptibility is shown in Fig. 2(b,c). There is no long-range order down to 0.42 K in both field directions below 1 T. The larger $H||ab$ magnetization indicates an easy-plane feature of $CsYbSe_2$, which is also found in other 112 compounds [39, 56]. A maximum is found in the temperature dependence of magnetization below 3 T for the $H||ab$. Since the heat capacity does not exhibit a λ anomaly in this temperature range, we suggest that the strong short-range interactions are developed. Zero-field cooled (ZFC) and field cooled (FC) susceptibility overlap at low temperatures (see inset in Fig. 2(b)), excluding the possibility of spin glass state. This behavior is different from that observed in $NaYbS_2$ single crystal, indicating a possible difference in the in-plane magnetism. It may be caused by the different distances between Yb^{3+}, spin-orbital coupling or different space groups. When the magnetic field reaches 3 T, an upturn is found at ~0.8 K, revealing the field-induced long-range magnetic order (LRO). As the magnetic field reaches 7 T, the magnetization shows a flat feature, indicating that the system moves to another magnetic state. Both LRO and maximum near 1.5 K were not found when a magnetic field up to 7 T is applied along the c axis due to the easy-plane anisotropy. The heat capacity measurements reveal the field-induced magnetic transition around 10 T, as we discuss in Section III B. Although a similar maximum is not found for the $H||c$, the observed deviation of the magnetic susceptibility from Curie-Weiss law below 8 K suggests that the crossover to QSL is present.

The effect of an applied field on the magnetization at different temperatures is shown in Fig. 3(a). The observed anisotropic ratio is larger than in $NaYbS_2$, which is consistent with the larger $d_{\rm inter}/d_{\rm NN}$ ratio in $CsYbSe_2$. We found an apparent magnetic plateau below T=1.2 K for the magnetic moment ~0.7 $\mu_{\rm B}$. From the theoretical calculations, the 1/3 magnetic plateau is expected in the easy-plane XXZ model [45]. Using the Curie-Weiss fitting at low temperature, we expect the g value of $g_{ab} = 4.0$ by assuming $S_{\rm eff}$=1/2. So, we estimate the saturation moment at low temperature $m_s = gJ$ to be 2 $\mu_{\rm B}$. The observed magnetic plateau is indeed close to 1/3 of the estimated saturation moment. There is no similar 1/3-

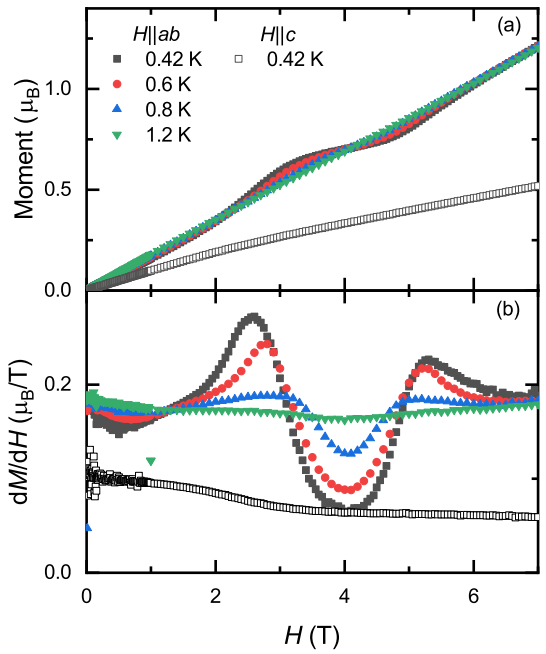

FIG. 3. Magnetization (a) and differential of magnetization (b) versus field for $H\|ab$ and $H\|c$ at different temperatures.

plateau on the magnetization curve in field $H||c$ up to 7 T. This is caused by the easy-plane anisotropy, which requires a higher magnetic field to build up a long-rang order along the c axis. The differential of the magnetization shows two peaks for the field direction $H\|ab$ (Fig. 3(b)). They become broader with temperature increasing but we still observe the anomalies at $T = 1.2$ K at 3 T and 5 T, indicating strong spin fluctuation. No peaks were found in the differential of magnetization for the field direction $H||c$ up to $H = 7$ T.

B. Heat Capacity

The zero-field heat capacity for $CsYbSe_2$ is shown in Fig. 4(a). The heat capacity goes to the Dulong-Petit limit of phonon contribution around 100 J/mol K [57]. A broad peak is found below 10 K, which is similar to that observed in the other Yb-112 materials implying the QSL states in the triangular Heisenberg lattices [42, 58, 59]. There is no λ anomaly around 1.5 K, confirming short-range correlations found in the magnetization. The broad peak moves slightly to high temperature in field H$\|c$ of 9 T (see Fig. 4(a)). The shift is smaller than that in $NaYbO_2$ powder, due to the easy-plane feature or large distance between the nearest neighbour Yb^{3+}.

To estimate the magnetic entropy, we subtract the phonon background using a nonmagnetic $CsLaSe_2$, as shown in Fig. 4(a). The integrated entropy is 5.4 J/mol

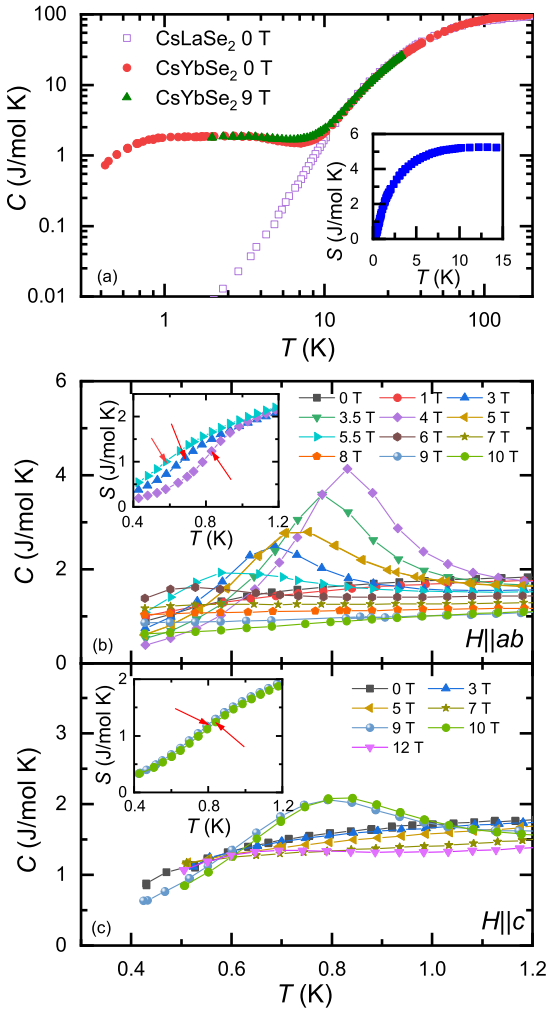

FIG. 4. (a) The temperature dependence of heat capacity of $CsYbSe_2$ and $CsLaSe_2$. The 9 T magnetic field is applied along the c axis. The inset presents the magnetic entropy of $CsYbSe_2$ below 15 K. (b,c) Low temperature specific heat of $CsYbSe_2$ under different magnetic fields for $H||ab$ (b) and $H||c$ (c). The inset shows the magnetic entropy of $CsYbSe_2$ in different magnetic fields below 1.2 K. The red arrow indicates the positions of LRO at each field.

K, which is 93% of the Rln2 of the spin-1/2 system. This result is consistent with the $S_{\rm eff}$=1/2 doublet in $CsYbSe_2$.

To investigate the field-induced magnetic phase transition, we measured the heat capacity in the field, in two directions $H||ab$ and $H||c$, at different temperatures, as shown in Fig. 4(b-c). When the small magnetic field was applied along the ab plane and the c axis, the heat capacity curves overlap very well, suggesting spin liquid behavior at the low magnetic fields. The field-induced magnetic transition is observed at $H = 3$ T when the magnetic field was applied along the ab plane, which is consistent with the magnetization measurements. The temperature and

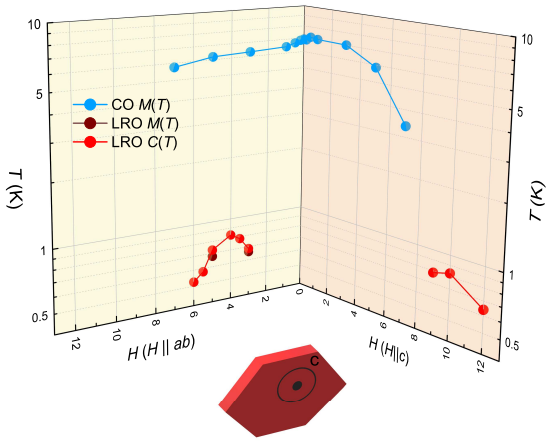

FIG. 5. Experimental H-T phase diagram of $CsYbSe_2$ obtained from heat capacity and magnetic susceptibility results. The values of the crossover (CO) are extracted as the temperature where magnetic susceptibility deviates from Curie-Weiss relation.

magnitude of the λ anomaly increase with the increasing of the magnetic field up to 4 T. The anomaly is sharpest at the highest transition temperature ~0.8 K, with a long tail above 1 K that indicates the large spin fluctuations. The magnetic transition is suppressed to a low temperature in fields $H||ab$ above 4 T and disappears at 7 T. The heat capacity at high magnetic field (>7 T) shows field-dependent relation and apparent difference from the low field ones (<3 T), indicating the different magnetic states in these two regions.

When increasing the $H||c$ magnetic field up to 9 T, a field-induced magnetic transition appears at 0.8 K that is similar to the case of $H||ab$ at 4 T. If we extend $M(H)$ to 9 T at $H||c$ and pick $M(H)$ at 3 T at $H||ab$, the estimated values of the magnetic moments at the magnetic transition are close in both directions. The magnetic field suppresses the transition to 0.6 K at 12 T and the clear difference was found at 3 T and 12 T above 0.6 K. This feature also indicates the different states induced by the high magnetic fields. The anisotropic heat capacity under magnetic fields is consistent with the magnetization measurements, suggesting the two-dimensional magnetism in $CsYbSe_2$ with the easy-plane anisotropy. The magnetic transition temperature in $CsYbSe_2$ is slightly lower than in the $NaYbO_2$. The integrated entropy in the vicinity of the LRO transition, as estimated in the inset of Fig. 4(b,c), is below 20% of Rln2, revealing strong spin fluctuation in $CsYbSe_2$.

Based on the magnetization and heat capacity results, in Fig. 5 we present a tentative H-T phase diagram for $CsYbSe_2$. Large magnetic anisotropy is clearly seen. The values of the crossover (CO) are extracted as the temperature where magnetic susceptibility deviates from Curie-Weiss relation. The LRO values obtained

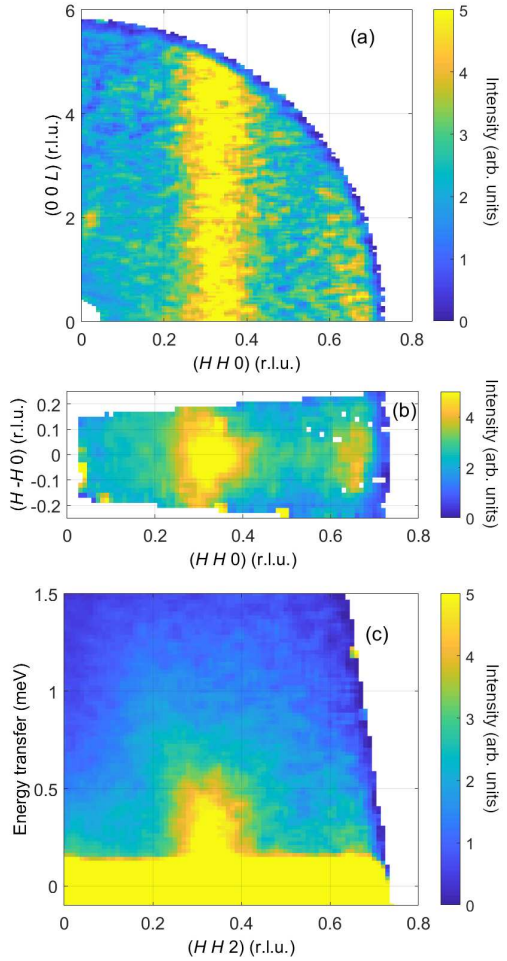

FIG. 6. (a,b) Constant energy plots in the (a^*c^*) plane (a) and the (a^*b^*) plane (b) at $T = 2$ K. The incident neutron energy is $E_i = 3.32$ meV. The scattering intensity was integrated within $\Delta E = [0.2, 0.4]$ meV. The data in (b) were symmetrized along the $(H$ -H 0) direction. Axis values are in reciprocal lattice units (r.l.u.). (c) Low-energy excitation spectrum of $CsYbSe_2$ at $T = 2$ K. Energy slice is taken along the $(HH2)$ direction with $(H$ -H 0) and (0 0 L) integrated over the range [-0.1, 0.1] and [1,4] r.l.u., respectively.

from heat capacity and magnetic susceptibility are consistent with each other. Note that the dome feature for LRO is also found in other frustrated magnetic materials [41, 42, 60, 61].

C. Inelastic Neutron Scattering

The eight-fold degenerate $J = 7/2$ ($L = 3$, $S = 1/2$) multiplet ($2J+1 = 8$) of Yb^{3+} is split into four Kramers doublet states. First, we probed for possible low-energy CEF excitations of the Yb^{3+} ions using neutron incident energy $E_i = 25$ meV. We did not find any excited CEF levels in the energy range below 20 meV (~230 K), which is in agreement with the results obtained for other

Yb-based triangle-lattice compounds, $YbMgGaO_4$ (E_1 = 38 meV) [29] and $NaYbS_2$ (E_1 = 23 meV) [39]. This is also in agreement with our heat capacity measurements where no Schottky anomaly is seen. Since the ground state is well separated from the other excited CEF levels, an effective spin-1/2 description is indeed appropriate at low temperature and magnetic properties are dominated by the ground-state Kramers doublet.

The experimental INS spectra for $CsYbSe_2$ are presented in Fig. 6 as false color plots of the neutron intensity without any background subtraction. Constant-energy slice in the (a^*c^*) plane, taken around energy E = 0.3 meV [Fig. 6(a)], shows clear intensity modulation along the (HH) direction. For the magnetic planes decoupled along c, the dispersion of the excitation would be expected to be independent of L. The data indeed indicate the absence of dispersion along L, implying that the inter-plane coupling is much weaker than the intra-plane correlations, in full agreement with the magnetization measurements.

The out-of-plane detector coverage of the CNCS TOF spectrometer is ±15°, so that a limited Q-range in the (a^*b^*) plane could also be accessed. Fig. 6(b) depicts the momentum dependence of an inelastic magnetic scattering for the energy range from 0.2 to 0.4 meV. Note that we symmetrized data along the (H -H 0) direction in order to get a large Q-coverage. The strongly dispersive scattering centered at the (1/3 1/3 0) point is clearly seen, suggesting a 120° non-collinear 2D-like spin correlations.

Fig. 6(c) illustrates the energy dependence of the scattering intensity along (H H) direction, which reveals broad excitations originated from the (1/3 1/3 L). The elastic scattering exhibits no magnetic Bragg peaks, confirming the absence of a long-range magnetic order. The excitations are gapless within the energy resolution and have a bandwidth of about 0.6 meV. In the highly degenerate spin-liquid ground state of our material, the magnetic excitations are over-damped away from the center of magnetic Brillouin zone, similar to the case of quantum spin-ice compound $Yb_2Ti_2O_7$ [62]. We note that the magnetic excitations in the $CsYbSe_2$ are in strong contrast to the data obtained for the other triangular-lattice compound $Ba_3CoSb_2O_9$, where well formed dispersion branches of single-magnon excitations and dispersive continua have been observed [50].

IV. CONCLUSION

Using the experimental results of magnetization, heat capacity and inelastic neutron scattering on $CsYbSe_2$ single crystals, we show that there is significant evidence to suggest that $CsYbSe_2$ provides a natural realization of the quantum spin liquid model at low magnetic fields. The magnetization and heat capacity show the absence of magnetic order and spin freezing down to T = 0.4 K at zero field. A magnetization plateau at one-third of the saturation magnetization is found at temperatures below 1.2 K, where temperature dependence of heat capacity confirms the magnetic field induced quantum phase transition. The central features of the observed inelastic magnetic scattering, that is the low-energy gapless over-damped 2D excitation centered at the (1/3 1/3 0) point, are the essential experimental hallmark of the S=1/2 triangular-lattice QSL. Our work also calls for further studies of the effects of magnetic field on the ground state and excitations, including mapping out dynamics in the 1/3-plateau. This requires larger single-crystal samples and INS measurements in field at ultra low temperatures and this work is in progress.

ACKNOWLEDGMENTS

We would like to thank D. Pajerowski and S. Nikitin for useful discussions. The research at the Oak Ridge National Laboratory (ORNL) is supported by the U.S. Department of Energy (DOE), Office of Science, Basic Energy Sciences (BES), Materials Sciences and Engineering Division. This research used resources at Spallation Neutron Source, a DOE Office of Science User Facility operated by ORNL. X-ray Laue alignment was conducted at the Center for Nanophase Materials Sciences (CNMS) (CNMS2019-R18) at ORNL, which is a DOE Office of Science User Facility. Work at Florida by J. S. Kim and G. R. S. supported by the US Department of Energy, Basic Energy Sciences, contract no. DE-FG02-86ER45268

[1] J.F. Sadoc and R. Mosseri, *Geometrical Frustration*, Collection Alea-Saclay: Monographs and Texts in Statistical Physics (Cambridge University Press, 1999).
[2] R. Moessner and A. P. Ramirez, "Geometrical frustration," Phys. Today **59**, 24–29 (2006).
[3] P.W. Anderson, "Resonating valence bonds: A new kind of insulator?" Mater. Res. Bull. **8**, 153 – 160 (1973).
[4] F. Mila, "Quantum spin liquids," Eur. J. Phys. **21**, 499–510 (2000).
[5] L. Balents, "Spin liquids in frustrated magnets," Nature **464**, 199–208 (2010).
[6] Y. Singh and P. Gegenwart, "Antiferromagnetic Mott insulating state in single crystals of the honeycomb lattice material Na_2IrO_3," Phys. Rev. B **82**, 064412 (2010).
[7] Y. Singh, S. Manni, J. Reuther, T. Berlijn, R. Thomale, W. Ku, S. Trebst, and P. Gegenwart, "Relevance of the Heisenberg-Kitaev Model for the Honeycomb Lattice Iridates A_2IrO_3," Phys. Rev. Lett. **108**, 127203 (2012).

[8] J. Chaloupka, G. Jackeli, and G. Khaliullin, "Kitaev-Heisenberg Model on a Honeycomb Lattice: Possible Exotic Phases in Iridium Oxides A_2IrO_3," Phys. Rev. Lett. **105**, 027204 (2010).

[9] I. I. Mazin, Harald O. Jeschke, Kateryna Foyevtsova, Roser Valentí, and D. I. Khomskii, "Na_2IrO_3 as a Molecular Orbital Crystal," Phys. Rev. Lett. **109**, 197201 (2012).

[10] F. Ye, S. Chi, H. Cao, B. C. Chakoumakos, J. A. Fernandez-Baca, R. Custelcean, T. F. Qi, O. B. Korneta, and G. Cao, "Direct evidence of a zigzag spin-chain structure in the honeycomb lattice: A neutron and x-ray diffraction investigation of single-crystal Na_2IrO_3," Phys. Rev. B **85**, 180403 (2012).

[11] T. Takayama, A. Kato, R. Dinnebier, J. Nuss, H. Kono, L. S. I. Veiga, G. Fabbris, D. Haskel, and H. Takagi, "Hyperhoneycomb Iridate $\beta-Li_2IrO_3$ as a Platform for Kitaev Magnetism," Phys. Rev. Lett. **114**, 077202 (2015).

[12] S. H. Chun, J.-W. Kim, J. Kim, H. Zheng, C. C. Stoumpos, C.D. Malliakas, J.F. Mitchell, K. Mehlawat, Y. Singh, Y. Choi, *et al.*, "Direct evidence for dominant bond-directional interactions in a honeycomb lattice iridate Na_2IrO_3," Nat. Phys. **11**, 462 (2015).

[13] K. Kitagawa, T. Takayama, Y. Matsumoto, A. Kato, R. Takano, Y. Kishimoto, S. Bette, R. Dinnebier, G. Jackeli, and H. Takagi, "A spin-orbital-entangled quantum liquid on a honeycomb lattice," Nature **554**, 341 (2018).

[14] C. Abramchuk, M.and Ozsoy-Keskinbora, J. W. Krizan, K. R. Metz, D. C. Bell, and F. Tafti, "Cu_2IrO_3: a new magnetically frustrated honeycomb iridate," J. Am. Chem. Soc. **139**, 15371–15376 (2017).

[15] T. Itou, A. Oyamada, S. Maegawa, M. Tamura, and R. Kato, "Quantum spin liquid in the spin-1/2 triangular antiferromagnet $EtMe_2Sb[Pd(dmit)_2]_2$," Phys. Rev. B **77**, 104413 (2008).

[16] A. Banerjee, C.A. Bridges, J.-Q. Yan, A.A. Aczel, L. Li, M.B. Stone, G.E. Granroth, M.D. Lumsden, Y. Yiu, J. Knolle, *et al.*, "Proximate Kitaev quantum spin liquid behaviour in a honeycomb magnet," Nat. Mater. **15**, 733 (2016).

[17] A. Banerjee, J. Yan, J. Knolle, C. A. Bridges, M. B. Stone, M. D. Lumsden, D. G. Mandrus, D. A. Tennant, R. Moessner, and S. E. Nagler, "Neutron scattering in the proximate quantum spin liquid α-RuCl3," Science **356**, 1055–1059 (2017).

[18] H. B. Cao, A. Banerjee, J.-Q. Yan, C. A. Bridges, M. D. Lumsden, D. G. Mandrus, D. A. Tennant, B. C. Chakoumakos, and S. E. Nagler, "Low-temperature crystal and magnetic structure of $\alpha-RuCl_3$," Phys. Rev. B **93**, 134423 (2016).

[19] K. Ran, J. Wang, W. Wang, Z.-Y. Dong, X. Ren, S. Bao, S. Li, Z. Ma, Y. Gan, Y. Zhang, J. T. Park, G. Deng, S. Danilkin, S.-Li Yu, J.-X. Li, and J. Wen, "Spin-Wave Excitations Evidencing the Kitaev Interaction in Single Crystalline $\alpha-RuCl_3$," Phys. Rev. Lett. **118**, 107203 (2017).

[20] I. A. Leahy, C. A. Pocs, Peter E. Siegfried, D. Graf, S.-H. Do, K.-Y. Choi, B. Normand, and M. Lee, "Anomalous Thermal Conductivity and Magnetic Torque Response in the Honeycomb Magnet $\alpha-RuCl_3$," Phys. Rev. Lett. **118**, 187203 (2017).

[21] L. S. Wu, S. E. Nikitin, Z. Wang, W. Zhu, C. D. Batista, A. M. Tsvelik, A. M. Samarakoon, D. A. Tennant, M. Brando, L. Vasylechko, M. Frontzek, A. T. Savici, G. Sala, G. Ehlers, A. D. Christianson, M. D. Lumsden, and A. Podlesnyak, "Tomonaga-Luttinger liquid behavior and spinon confinement in $YbAlO_3$," Nat. Commun. **10**, 698 (2019).

[22] L. S. Wu, S. E. Nikitin, M. Brando, L. Vasylechko, G. Ehlers, M. Frontzek, A. T. Savici, G. Sala, A. D. Christianson, M. D. Lumsden, and A. Podlesnyak, "Antiferromagnetic ordering and dipolar interactions of $YbAlO_3$," Phys. Rev. B **99**, 195117 (2019).

[23] C. E. Agrapidis, J. van den Brink, and S. Nishimoto, "Field-induced incommensurate ordering in Heisenberg chains coupled by Ising interaction: Model for ytterbium aluminum perovskite $YbAlO_3$," Phys. Rev. B **99**, 224423 (2019).

[24] G. Hester, H. S. Nair, T. Reeder, D. R. Yahne, T. N. DeLazzer, L. Berges, D. Ziat, J. R. Neilson, A. A. Aczel, G. Sala, J. A. Quilliam, and K. A. Ross, "Novel Strongly Spin-Orbit Coupled Quantum Dimer Magnet: $Yb_2Si_2O_7$," Phys. Rev. Lett. **123**, 027201 (2019).

[25] Y. Li, H. Liao, Z. Zhang, S. Li, F. Jin, L. Ling, L. Zhang, Y. Zou, Li Pi, Z. Yang, *et al.*, "Gapless quantum spin liquid ground state in the two-dimensional spin-1/2 triangular antiferromagnet $YbMgGaO_4$," Scientific reports **5**, 16419 (2015).

[26] Y. Li, G. Chen, W. Tong, Li Pi, J. Liu, Z. Yang, X. Wang, and Q. Zhang, "Rare-Earth Triangular Lattice Spin Liquid: A Single-Crystal Study of $YbMgGaO_4$," Phys. Rev. Lett. **115**, 167203 (2015).

[27] Y. Li, D. Adroja, P. K. Biswas, P. J. Baker, Q. Zhang, J. Liu, A. A. Tsirlin, P. Gegenwart, and Q. Zhang, "Muon Spin Relaxation Evidence for the U(1) Quantum Spin-Liquid Ground State in the Triangular Antiferromagnet $YbMgGaO_4$," Phys. Rev. Lett. **117**, 097201 (2016).

[28] Y. Shen, Y.-D. Li, H. Wo, Y. Li, S. Shen, B. Pan, Q. Wang, H.C. Walker, P. Steffens, M. Boehm, *et al.*, "Evidence for a spinon Fermi surface in a triangular-lattice quantum-spin-liquid candidate," Nature **540**, 559 (2016).

[29] J. A. M. Paddison, M. Daum, Z. Dun, G. Ehlers, Y. Liu, M. B. Stone, H. Zhou, and M. Mourigal, "Continuous excitations of the triangular-lattice quantum spin liquid $YbMgGaO_4$," Nat. Phys. **13**, 117 (2017).

[30] X. Zhang, F. Mahmood, M. Daum, Z. Dun, J. A. M. Paddison, N. J. Laurita, T. Hong, H. Zhou, N. P. Armitage, and M. Mourigal, "Hierarchy of Exchange Interactions in the Triangular-Lattice Spin Liquid $YbMgGaO_4$," Phys. Rev. X **8**, 031001 (2018).

[31] Y. Li, D. Adroja, R. I. Bewley, D. Voneshen, A. A. Tsirlin, P. Gegenwart, and Q. Zhang, "Crystalline Electric-Field Randomness in the Triangular Lattice Spin-Liquid $YbMgGaO_4$," Phys. Rev. Lett. **118**, 107202 (2017).

[32] W. M. Steinhardt, Z. Shi, A. Samarakoon, S. Dissanayake, D. Graf, Y. Liu, W. Zhu, C. Marjerrison, C. D. Batista, and S. Haravifard, "Field-Induced Phase Transition of the Spin Liquid State in Triangular Antiferromagnet $YbMgGaO_4$," arXiv preprint arXiv:1902.07825 (2019).

[33] Y. Shen, Y.-D. Li, H.C. Walker, P. Steffens, M. Boehm, X. Zhang, S. Shen, H. Wo, G. Chen, and J. Zhao, "Fractionalized excitations in the partially magnetized spin liquid candidate $YbMgGaO_4$," Nat. Commun. **9**, 4138 (2018).

[34] Z. Zhu, P. A. Maksimov, S. R. White, and A. L. Chernyshev, "Disorder-Induced Mimicry of a Spin Liquid in $YbMgGaO_4$," Phys. Rev. Lett. **119**, 157201 (2017).

[35] Z. Zhu, P. A. Maksimov, S. R. White, and A. L. Chernyshev, "Topography of Spin Liquids on a Triangular Lattice," Phys. Rev. Lett. **120**, 207203 (2018).

[36] I. Kimchi, A. Nahum, and T. Senthil, "Valence Bonds in Random Quantum Magnets: Theory and Application to $YbMgGaO_4$," Phys. Rev. X **8**, 031028 (2018).

[37] Weiwei L., Zheng Z., Jianting Ji, Yixuan L., Jianshu Li, Xiaoqun W., Hechang L., Gang C., and Qingming Z., "Rare-Earth Chalcogenides: A Large Family of Triangular Lattice Spin Liquid Candidates," Chinese Phys. Lett. **35**, 117501 (2018).

[38] Z. Zangeneh, S. Avdoshenko, J. Brink, and L. Hozoi, "Single-site magnetic anisotropy governed by inter-layer cation charge imbalance in triangular-lattice $AYbX_2$," arXiv preprint arXiv:1909.01224 (2019).

[39] M. Baenitz, Ph. Schlender, J. Sichelschmidt, Y. A. Onykiienko, Z. Zangeneh, K. M. Ranjith, R. Sarkar, L. Hozoi, H. C. Walker, J.-C. Orain, H. Yasuoka, J. van den Brink, H. H. Klauss, D. S. Inosov, and Th. Doert, "$NaYbS_2$: A planar spin-1/2 triangular-lattice magnet and putative spin liquid," Phys. Rev. B **98**, 220409 (2018).

[40] L. Ding, P. Manuel, S. Bachus, F. Grußler, Ph. Gegenwart, J. Singleton, R. D. Johnson, H. C. Walker, D. T. Adroja, A. D. Hillier, *et al.*, "Gapless spin-liquid state in the structurally disorder-free triangular antiferromagnet $NaYbO_2$," arXiv preprint arXiv:1901.07810 (2019).

[41] K. M. Ranjith, D. Dmytriieva, S. Khim, J. Sichelschmidt, S. Luther, D. Ehlers, H. Yasuoka, J. Wosnitza, A. A. Tsirlin, H. Kühne, and M. Baenitz, "Field-induced instability of the quantum spin liquid ground state in the $J_{\rm eff} = \frac{1}{2}$ triangular-lattice compound $NaYbO_2$," Phys. Rev. B **99**, 180401 (2019).

[42] M. Bordelon, E. Kenney, T. Hogan, L. Posthuma, M. Kavand, Y. Lyu, M. Sherwin, C. Brown, M.J. Graf, L. Balents, *et al.*, "Field-tunable quantum disordered ground state in the triangular lattice antiferromagnet $NaYbO_2$," arXiv preprint arXiv:1901.09408 (2019).

[43] D. A. Huse and V. Elser, "Simple Variational Wave Functions for Two-Dimensional Heisenberg Spin-1/2 Antiferromagnets," Phys. Rev. Lett. **60**, 2531–2534 (1988).

[44] A. V. Chubokov and D. I. Golosov, "Quantum theory of an antiferromagnet on a triangular lattice in a magnetic field," J. Phys. Condens. Matter **3**, 69–82 (1991).

[45] D. Yamamoto, G. Marmorini, and I. Danshita, "Quantum Phase Diagram of the Triangular-Lattice XXZ Model in a Magnetic Field," Phys. Rev. Lett. **112**, 127203 (2014).

[46] T. Ono, H. Tanaka, H. Aruga K., F. Ishikawa, H. Mitamura, and T. Goto, "Magnetization plateau in the frustrated quantum spin system Cs_2CuBr_4," Phys. Rev. B **67**, 104431 (2003).

[47] N. Terada, Y. Narumi, K. Katsumata, T. Yamamoto, U. Staub, K. Kindo, M. Hagiwara, Y. Tanaka, A. Kikkawa, H. Toyokawa, T. Fukui, R. Kanmuri, T. Ishikawa, and H. Kitamura, "Field-induced lattice staircase in a frustrated antiferromagnet $CuFeO_2$," Phys. Rev. B **74**, 180404 (2006).

[48] Y. Shirata, H. Tanaka, A. Matsuo, and K. Kindo, "Experimental Realization of a Spin-1/2 Triangular-Lattice Heisenberg Antiferromagnet," Phys. Rev. Lett. **108**, 057205 (2012).

[49] M. Lee, J. Hwang, E. S. Choi, J. Ma, C. R. Dela Cruz, M. Zhu, X. Ke, Z. L. Dun, and H. D. Zhou, "Series of phase transitions and multiferroicity in the quasi-two-dimensional spin-$\frac{1}{2}$ triangular-lattice antiferromagnet $Ba_3CoNb_2O_9$," Phys. Rev. B **89**, 104420 (2014).

[50] S. Ito, N. Kurita, H. Tanaka, S. Ohira-Kawamura, K. Nakajima, S. Itoh, K. Kuwahara, and K. Kakurai, "Structure of the magnetic excitations in the spin-1/2 triangular-lattice Heisenberg antiferromagnet $Ba_3CoSb_2O_9$," Nat. Commun. **8**, 235 (2017).

[51] J. Xing, L. D. Sanjeewa, J. Kim, G.R. Stewart, M.-H. Du, F. A. Reboredo, R. Custelcean, and A. S. Sefat, ACS Materials Lett. , 71–75 (2019).

[52] G. Ehlers, A. Podlesnyak, J. L. Niedziela, E. B. Iverson, and P. E. Sokol, "The new cold neutron chopper spectrometer at the spallation neutron source: design and performance," Rev. Sci. Instrum. **82**, 085108 (2011).

[53] G. Ehlers, A. Podlesnyak, and A. I. Kolesnikov, "The cold neutron chopper spectrometer at the Spallation Neutron Source - A review of the first 8 years of operation," Rev. Sci. Instrum. **87**, 093902 (2016).

[54] O. Arnold, J. C. Bilheux, J. M. Borreguero, A. Buts, S. I. Campbell, L. Chapon, M. Doucet, N. Draper, R. F. Leal, M. A. Gigg, *et al.*, "Mantid – Data analysis and visualization package for neutron scattering and μSR experiments," Nucl. Instrum. Methods Phys. Res. Sect. A **764**, 156 (2014).

[55] R. A. Ewings, A. Buts, M. D. Le, J. van Duijn, I. Bustinduy, and T. G. Perring, "HORACE: software for the analysis of data from single crystal spectroscopy experiments at time-of-flight neutron instruments," Nucl. Instrum. Methods Phys. Res. Sect. A **834**, 3132–142 (2016).

[56] Jie Xing, Liurukara D. Sanjeewa, Jungsoo Kim, William R. Meier, Andrew F. May, Qiang Zheng, Radu Custelcean, G. R. Stewart, and Athena S. Sefat, "Synthesis, magnetization, and heat capacity of triangular lattice materials $naerse_2$ and $kerse_2$," Phys. Rev. Materials **3**, 114413 (2019).

[57] Charles Kittel, "Solid state physics," Wiley, New York **19** (1976).

[58] Y. R. Wang, "Specific heat of quantum Heisenberg model on a triangular lattice with two exchange parameters and its application to ^{3}He adsorbed on graphite," Phys. Rev. B **45**, 12608–12611 (1992).

[59] M. Isoda, H. Nakano, and T. Sakai, "Specific Heat and Magnetic Susceptibility of Ising-Like Anisotropic Heisenberg Model on Kagome Lattice," J. Phys. Soc. Jpn. **80**, 084704 (2011).

[60] G. Quirion, M. Lapointe-Major, M. Poirier, J. A. Quilliam, Z. L. Dun, and H. D. Zhou, "Magnetic phase diagram of $Ba_3CoSb_2O_9$ as determined by ultrasound velocity measurements," Phys. Rev. B **92**, 014414 (2015).

[61] K. M. Ranjith, S. Luther, T. Reimann, B. Schmidt, Ph. Schlender, J. Sichelschmidt, H. Yasuoka, A. M. Strydom, Y. Skourski, J. Wosnitza, H. Khne, Th. Doert, and M. Baenitz, "Anisotropic field-induced ordering in the triangular-lattice quantum spin liquid $NaYbSe_2$," arXiv preprint arXiv:1911.12712 (2019).

[62] K. A. Ross, J. P. C. Ruff, C. P. Adams, J. S. Gardner, H. A. Dabkowska, Y. Qiu, J. R. D. Copley, and B. D. Gaulin, "Two-Dimensional Kagome Correlations and Field Induced Order in the Ferromagnetic XY Pyrochlore $Yb_2Ti_2O_7$," Phys. Rev. Lett. **103**, 227202 (2009).